J. Fluid Mech. (2008), *vol.* 595, *pp.* 367–377. © 2008 Cambridge University Press
doi:10.1017/S0022112007009159 Printed in the United Kingdom

Nonlinear global modes in inhomogeneous mixed convection flows in porous media

M. N. OUARZAZI[1], F. MEJNI[1], A. DELACHE[1] AND G. LABROSSE[2]

[1]Laboratoire de Mécanique de Lille, UMR CNRS 8107, USTL, bd. Paul Langevin 59655 Villeneuve d'Ascq cedex, France

[2]Université Paris Sud, Limsi-CNRS, Bâtiments 508 et 502, 91403 Orsay, France

(Received 3 July 2007 and in revised form 22 September 2007)

The aim of this work is to investigate the fully nonlinear dynamics of mixed convection in porous media heated non-uniformly from below and through which an axial flow is maintained. Depending on the choice of the imposed inhomogeneous temperature profile, two cases prove to be of interest: the base flow displays an absolute instability region either detached from the inlet or attached to it. Results from a combined direct numerical simulations and linear stability approach have revealed that in the first case, the nonlinear solution is a steep nonlinear global mode, with a sharp stationary front located at a marginally absolutely unstable station. In the second configuration, the scaling laws for the establishment of a nonlinear global mode quenched by the inlet are found to agree perfectly with the theory. It is also found that in both configurations, the global frequency of synchronized oscillations corresponds to the local absolute frequency determined by linear criterion, even far from the threshold of global instability.

1. Introduction

During the last few decades significant advances have been made in the theory of nonlinear global modes dealing with spatially developing flows (for a recent review see Chomaz 2005). The method of reducing complicated problems into simple models retaining only the most essential features turns out to be very successful. Specifically, in a semi-infinite medium $x > 0$, Couairon & Chomaz (1999) studied the nonlinear solutions of the supercritical Landau–Ginzburg amplitude equation, with spatially varying coefficients and with the condition of vanishing amplitude at the inlet. They showed that the solutions called nonlinear global modes are associated with a pulled front selected by a linear criterion. The selected frequency near the onset of global instability is found to correspond to the absolute frequency at the inlet of the medium. They also derived scaling laws of the amplitude of nonlinear global modes and for the position of its maximum. In connection with real open-flow systems, the derived scaling laws have been shown to agree well with the experimental observations of Goujon-Durand, Jenffer & Wesfreid (1994) and with the numerical simulations of Zielinska & Wesfreid (1995) of the wake behind bluff bodies. As for the infinite domain, Pier, Huerre & Chomaz (2001) analysed the properties of fully nonlinear self-sustained global modes in the framework of supercritical complex Landau–Ginzburg amplitude equations with slowly spatially varying coefficients. When the base flow displays a finite pocket of absolute instability

https://doi.org/10.1017/S0022112007009159 Published online by Cambridge University Press

within the medium, steep global modes were identified and are characterized by a sharp stationary front located at the upstream boundary of absolute instability which imposes its local absolute frequency on the entire medium. The analytical structure underlying the spatial distribution of steep global modes has been analysed in a consistent manner by using a matched asymptotic expansion method (Pier *et al.* 2001). The derived selection principle of the self-sustained synchronized oscillations of steep global modes has been confirmed by direct simulations of real physical systems such as two-dimensional wakes (Pier & Huerre 2001), separated boundary-layer flow over a double-bump geometry (Marquillie & Ehrenstein 2003) and hot jets (Lesshafft *et al.* 2006).

The objective of the present investigation is to study the interplay between localization, advection, instability and nonlinearity for natural convection forced by a horizontal pressure gradient in porous media, a problem generally termed the mixed convection problem. Our first motivation is to compare our findings stemming from the combined direct numerical simulations and linear stability approach to the theory of global modes in both semi-infinite and infinite domains. The second motivation follows from experimental studies of natural convection in porous media conducted by Shattuck *et al.* (1997) and Howle, Behringer & Georgiadis (1997). In general, it is found that the structure of the porous medium plays a role which is not predicted by theories which assume a homogeneous system. Stable localized patterns were observed in regions with locally larger permeability, and hence larger local filtration Rayleigh number. By analogy, larger local filtration Rayleigh number is conceived here by imposing an inhomogeneous temperature profile on the bottom plate. In the case of homogeneous heating, the linear analysis presented by Delache, Ouarzazi & Combarnous (2007) allowed discrimination between the convective and absolute nature of the instability of the basic flow. In relation to experiments conducted by Combarnous & Bories (1975), Delache *et al.* (2007) found that the border between the convective and the absolute instability in the filtration Rayleigh–Péclet number plane corresponds perfectly to the experimentally observed transition to oscillatory transversal rolls.

The outline of the study is as follows. The equations governing the problem together with the steady state and its linear stability are presented in § 2. After a short description of the numerical method, the nonlinear global modes are computed by direct numerical simulations of the coupled Darcy's and energy equations. The corresponding properties are presented and compared to the theory of nonlinear global modes in the case of infinite media in § 3.1 and for semi-infinite media in § 3.2. The main results of the study are summarized in § 4.

2. Problem formulation, steady-state and linear theory

We consider an isotropic and homogeneous porous layer of rectangular cross-section with thickness H and width aH when the temperature of the bottom wall exceeds that of the upper boundary and is modulated on a length scale $L \gg H$. We denote the ratio H/L by ε and assume that $\varepsilon \ll 1$. The lateral boundaries are assumed impermeable and perfectly heat insulating. Furthermore, we consider that a through-flow is driven by a pressure gradient in the x-direction. We choose H, $H^2(\rho c)/k_{stg}$, $k_{stg}/(H(\rho c)_f)$ and $k_{stg}\mu/(K(\rho c)_f)$ as references for length, time, filtration velocity and pressure. Here, k_{stg}, (ρc), $(\rho c)_f$, K and μ are, respectively, the effective stagnant thermal conductivity, the overall heat capacity of the porous medium per unit volume, the heat capacity per unit volume of the fluid alone, the permeability of the medium

https://doi.org/10.1017/S0022112007009159 Published online by Cambridge University Press

and the viscosity of the fluid. The temperature T^* is made dimensionless by writing $T^* = T_1^* + (\Delta T)T$, where T_1^* is the temperature of the upper boundary and ΔT is the maximum temperature difference between the boundaries. Darcy's law is used and the Boussinesq approximation is employed. Under these conditions the dimensionless equations governing the flow are:

$$\nabla \cdot \boldsymbol{V} = 0, \tag{2.1}$$

$$\boldsymbol{V} + \nabla P - Ra T \boldsymbol{e}_z = 0, \tag{2.2}$$

$$\partial_t T + \boldsymbol{V} \cdot \nabla T - \nabla^2 T = 0, \tag{2.3}$$

with boundary conditions:

$$\boldsymbol{V} \cdot \boldsymbol{e}_z = 0 \text{ at } z = 0, 1; \ \boldsymbol{V} \cdot \boldsymbol{e}_y = 0 \text{ at } y = 0, a, \tag{2.4}$$

$$T(z=0) = 1 - F(X = \varepsilon x) \leqslant 1; \ T(z=1) = 0; \ \partial T/\partial y = 0 \text{ at } y = 0, a, \tag{2.5}$$

with an imposed through-flow:

$$\int_0^1 \boldsymbol{V} \cdot \boldsymbol{e}_x \, \mathrm{d}z = Pe. \tag{2.6}$$

The system is characterized by the following dimensionless parameters: the filtration Rayleigh number $Ra = K g \alpha H \Delta T (\rho c)_f / k_{stg} \nu$, the Péclet number $Pe = UH(\rho c)_f / k_{stg}$, the lateral aspect ratio a and the small parameter ε.

U, g , ν, α and C are, respectively, the average filtration velocity imposed at the entrance of the channel, the acceleration due to gravity, the kinematic viscosity and the volumetric coefficient of thermal expansion.

Our aim is first to find an approximation to the steady-state solution, then to examine its spatio-temporal linear stability and finally to perform direct numerical two-dimensional simulations to characterize some properties of the nonlinear solution. We search for a steady-state solution with $(u, v, w, T, P) = (\boldsymbol{u}_B, 0, \boldsymbol{w}_B, \boldsymbol{T}_B, \boldsymbol{P}_B)$ of (2.1)–(2.3) with boundary conditions (2.4)–(2.6). After some, not altogether trivial, work we find a consistent expansion in the form:

$$\boldsymbol{T}_B = (1-z)(1-F) + \varepsilon \, Pe \left(\frac{z}{3} - \frac{z^2}{2} + \frac{z^3}{6} \right) \partial_X F + o(\varepsilon), \tag{2.7}$$

$$\boldsymbol{u}_B = Pe - \varepsilon \, Ra \left(\frac{1}{3} - z + \frac{z^2}{2} \right) \partial_X F + o(\varepsilon), \tag{2.8}$$

$$\boldsymbol{w}_B = \varepsilon^2 Ra \left(\frac{z}{3} - \frac{z^2}{2} + \frac{z^3}{6} \right) \partial_X^2 F + o(\varepsilon^2), \tag{2.9}$$

$$\boldsymbol{P}_B = -Pe \, x + Ra \left(z - \frac{z^2}{2} \right) + Ra \, F(X) \left(\frac{1}{3} - z + \frac{z^2}{2} \right) + O(\varepsilon). \tag{2.10}$$

Linearizing the system (2.1)–(2.3) around the basic solution (2.7)–(2.10) introduces two horizontal length scales, and analytic solutions may be obtained in the framework of the WKBJ approximation. The three-dimensional infinitesimal perturbations verifying the boundary conditions are then expressed as

https://doi.org/10.1017/S0022112007009159 Published online by Cambridge University Press

$$\begin{pmatrix} u \\ v \\ w \\ \theta \\ p \end{pmatrix} = \exp\left(\frac{\mathrm{i}}{\varepsilon}\int k(X)\mathrm{d}X - \mathrm{i}\omega_0 t\right) \begin{pmatrix} u_1(X)\cos[\pi z]\cos[(m/a)\pi y] \\ v_1(X)\cos[\pi z]\sin[(m/a)\pi y] \\ w_1(X)\sin[\pi z]\cos[(m/a)\pi y] \\ \theta_1(X)\sin[\pi z]\cos[(m/a)\pi y] \\ p_1(X)\cos[\pi z]\cos[(m/a)\pi y] \end{pmatrix} + \text{c.c.}, \quad (2.11)$$

where ω_0 and k are the complex frequency and the longitudinal wavenumber, respectively, $m\pi/a$ being the real wavenumber in the spanwise direction.

If we substitute (2.11) into the equations of motion (2.1)–(2.3), linearized around the base flow, we obtain at leading order an algebraic system with a non-trivial solution only if the problem is singular, which implies an explicit dispersion relation:

$$D(\omega_0, k, X, m, a, Ra, Pe) = \left(k^2 + \pi^2(1 + m^2/a^2)\right)$$
$$(-\mathrm{i}\omega_0 + \mathrm{i}kPe + k^2 + \pi^2(1 + m^2/a^2)) - (k^2 + \pi^2 m^2/a^2)Ra(1 - F(X)) = 0. \quad (2.12)$$

We emphasize that our main objective is to compare the local absolute frequencies to the global frequencies computed by direct numerical simulations. Therefore we are not interested in the present study by the analytical construction of the linear global mode, i.e. by the determination of the five functions of X in (2.11). This analytical construction is mathematically similar to that performed by Monkewitz, Huerre & Chamaz (1993) and Ouarzazi, Bois & Taki (1996) and is postponed to a subsequent paper. Here, we briefly recall that in the unstable case, if $\partial_k\omega_0 = 0$, a perturbation at fixed x grows with a rate $\omega_{0,i}(k)$. When $\omega_{0,i}(k)$ is positive, the system is said to be absolutely unstable and localized perturbations grow *in situ* and also expand in space. On the other hand, if $\omega_{0,i}(k)$ is negative, the system is said to be convectively unstable, meaning that any localized impulse is convected away so that instabilities cannot globally grow. In order to investigate the roll orientation corresponding to the highest local absolute growth rate $\omega_{0,i}(k, X, m)$, we solve the following system by means of a Newton–Raphson algorithm : $D(\omega_0, k, X, m, a, Ra, Pe) = 0$ and $\mathrm{d}\omega_0/\mathrm{d}k = 0$.

The dependence on Ra and Pe of $\omega_{0,i}(k, X, m)$ is determined for different m. We found that the mode $m = 0$ corresponding to oscillatory pure transverse rolls is the most amplified mode in the absolutely unstable parameter range studied. We have checked that this pattern selection related to the highest local absolute growth rate remains pertinent for any lateral aspect ratio a. In the limit of infinite a, this pattern selection has been shown to also hold in the Poiseuille–Rayleigh-Bénard problem (Carrière & Monkewitz 1999). We therefore restrict, in the remainder of this paper, the investigation of linear and nonlinear properties to transverse rolls. We wish to make it clear that the present two-dimensional investigation is justified if it is assumed that the temperature of the bottom wall is only inhomogeneous in the x-direction and the sidewalls are perfectly heat insulating. In more realistic configurations with inhomogeneities also acting in the y-direction and where the sidewalls are not thermally insulated, the dynamics is complicated and three-dimensional instabilities other than pure transverse rolls may be the most amplified. Depending on the choice of the imposed inhomogeneous temperature profile, two generic configurations are considered. The first configuration, adapted to infinite media, is built such that the streamwise development of $\omega_{0,i}(k, X, m = 0)$ presents a local maximum within the medium and decays upstream and downstream. In contrast, the second configuration adequate to semi-infinite media is conceived to allow $\omega_{0,i}(k, X, m = 0)$ to decrease continuously from the entrance cross-section of the

https://doi.org/10.1017/S0022112007009159 Published online by Cambridge University Press

channel. The streamwise dependence of the frequency $\omega_{0,r}(X)$ is displayed in figure 1(*a*) for $Pe = 6$ and $Ra = 60$ in the case of infinite media. The shape of the inhomogeneous temperature imposed at the lower boundary, namely $T(z = 0) = 1 - \tanh^2(X)$, allows the base flow to display a region of absolute instability extending from the location x_{ca} to the spatial position x_{ac}. Below x_{ca} (beyond x_{ac}), the flow is convectively unstable until the station x_{sc} (x_{cs}), where a transition to a stable region occurs. Corresponding variations of local frequencies for semi-infinite media are shown in figure 1(*b*) for $Pe = 5$ and $Ra = 52$. The local absolute instability of the base flow extending from the inlet to x_{ac} is generated by the choice $T(z = 0) = 1 - \tanh(X)$. Beyond x_{ac}, the flow is convectively unstable until x_{cs}, where a transition to a stable region occurs.

According to the theory of nonlinear global modes (Chomaz 2005), an interesting issue related to the global frequency selection criterion is the evolution of both the marginal absolute frequency $\omega_0^{ca} = \omega_{0,r}(x = x_{ca})$ in the case of infinite media and the absolute frequency $\omega_{0,r}(x = 0)$ at the inlet of semi-infinite media. The marginal absolute frequency is sketched in figure 1(*c*) for $Pe = 6$ with variable Ra and in figure 1(*e*) for variable Pe and $Ra = 65$. Similarly, the variations of $\omega_{0,r}(x = 0)$ as functions of Ra and Pe are shown in figures 1(*d*) and 1(*f*), respectively.

The purpose of the following section is to perform direct numerical two-dimensional simulations of the problem, the results of which will be compared to linear theory.

3. Nonlinear global modes and comparison with linear theory

The two-dimensional mixed convection problem in porous medium, (2.1)–(2.3), is numerically solved using a pseudospectral method in space: the unknown fields, $\boldsymbol{V}$, P and T, are expanded in Chebyshev polynomials in both x- and z-directions. The energy equation (2.3) is discretized by a scheme of second-order temporal accuracy, with an implicit Euler scheme on the diffusion term, and an explicit Adams–Bashforth scheme for the convective contribution. The code used is an extension of a code designed for solving the Navier–Stokes equations for fluids flowing in closed cavities. Its specificity relies on an efficient two-dimensional/three-dimensional Stokes solver shown by Leriche & Labrosse (2000) as being consistent with the continuous problem. This code has been used with many different physical configurations, for instance for the Stokes eigenmodes dynamics (Leriche & Labrosse 2007). The first step of this Stokes solver is a Darcy solver supplying an exact divergence-free velocity field. The code was adapted with (i) a by-pass of the Stokes solver second step, (ii) the treatment of an open flow configuration and (iii) the addition of the energy equation. The computational domains are either $[-L, L]$ for the case of a pocket of absolute instability within the medium, or $[0, L]$ if the base flow is absolutely unstable at the inlet. In order to avoid outflow effects, the computational domains are chosen so that the base flow is always stable in a finite region near the outlet. To simulate the axial flow through the porous sidewalls in the x-direction, a uniform horizontal velocity profile is assumed and the conductive temperature profile $(1 - z)(1 - F)$ is imposed. The initial conditions for the velocity and the temperature are taken to be the basic state approximated by (2.7)–(2.9) plus a perturbation. The numerical solution supplies the total field, from which the perturbation field is extracted by removing the basic state. As a validation test, the results of Dufour & Néel (1998) for the homogeneous heating case have been successfully reproduced.

3.1. *Results for nonlinear global mode with a pocket of absolute instability*

The first simulation is carried out with $Ra = 60$, $Pe = 6$ and $\varepsilon = 0.01$. Figure 2(*a*) illustrates the obtained nonlinear global mode solution in the asymptotic state,

https://doi.org/10.1017/S0022112007009159 Published online by Cambridge University Press

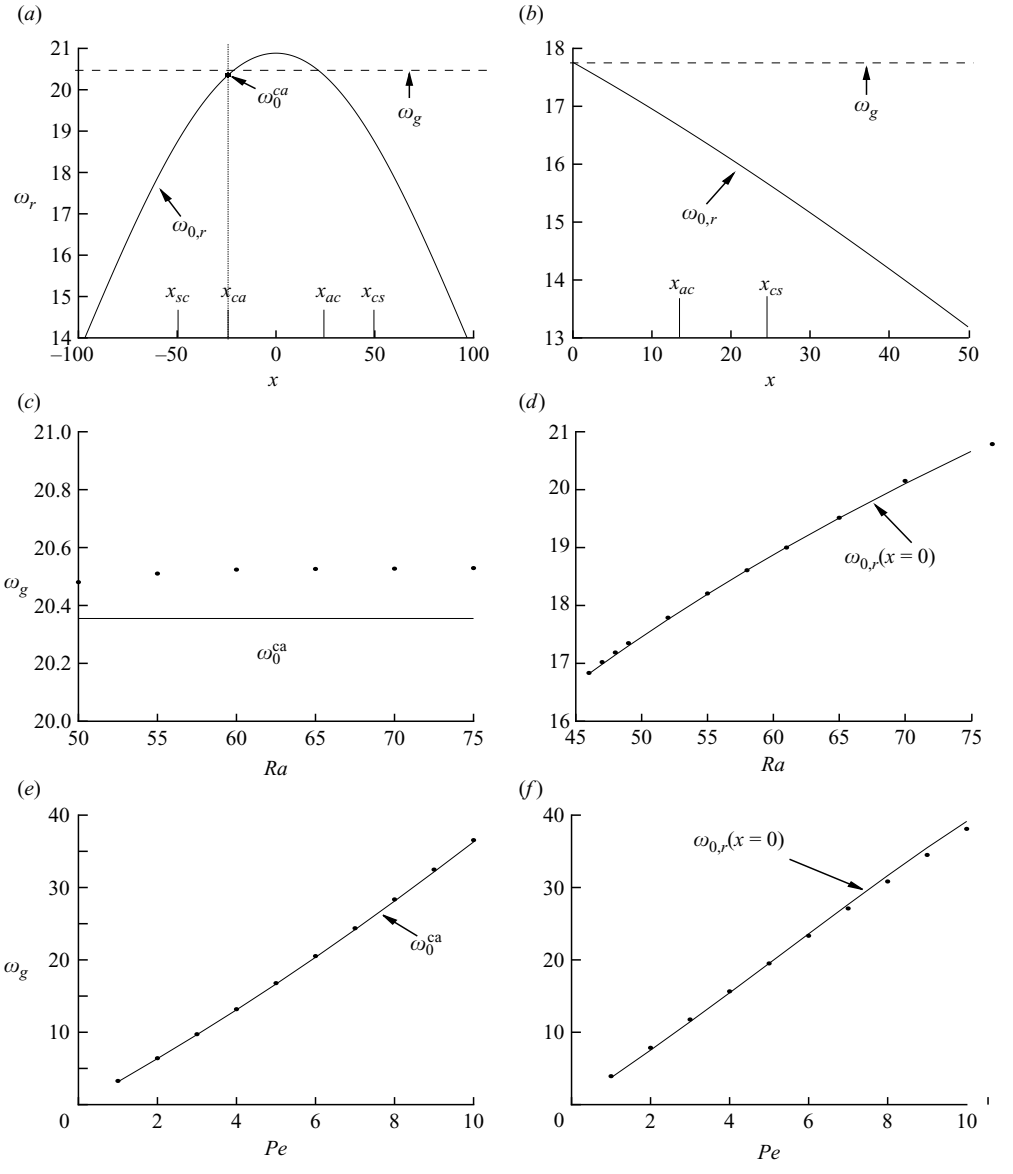

FIGURE 1. Comparison of the numerically observed global frequency ω_g (dashed or dotted) with results obtained from linear theory (solid) for infinite (*a, c, e*) and semi-infinite (*b, d, f*) domains. Local absolute frequency as a function of streamwise coordinate x for (*a*) $Pe=6$ and $Ra=60$ and (*b*) $Pe=5$ and $Ra=52$. Marginal absolute frequency ω_0^{ca} for (*c*) $Pe=6$ and varying Ra and (*e*) varying Pe and $Ra=65$. Absolute frequency at the inlet for (*d*) $Pe=5$ and varying Ra and $Ra=52$ and varying Pe.

characterized by a sharp front located at the upstream boundary x_{ca} of the absolute unstable region. This spatial structure points to the need to ascertain that the observed nonlinear global mode is a steep one according to principles proposed by Pier *et al.* (2001). This task will be accomplished through a series of suitable numerical experiments to test the following features of steep nonlinear global modes: (i) that the global frequency is simply determined by ω_0^{ca} obtained by linear dispersion equation;

https://doi.org/10.1017/S0022112007009159 Published online by Cambridge University Press

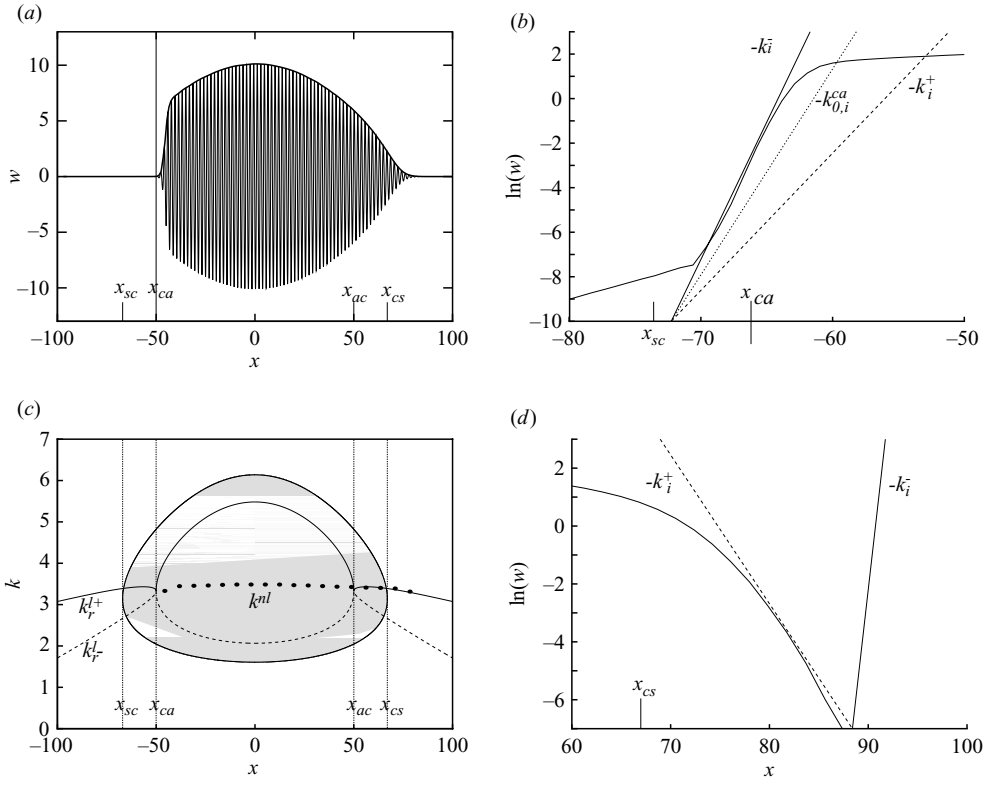

FIGURE 2. (*a*) Nonlinear global mode shape for infinite domain; the perturbation of the vertical velocity component in the middle of the porous medium is presented as a function of the downstream distance for $Pe = 6$, $Ra = 60$ and $\epsilon = 0.01$. (*b*) Semi-algorithmic plot of the upstream front; comparison of the front slope with spatial growth rates $-k_i^-(\omega_0^{ca}, x = -55) = 1.99$, $-k_{0,i}^{ca} = 1.3$ and $-k_i^+(\omega_0^{ca}, x = -55) = 0.6$. (*d*) Semi-algorithmic plot of the decaying nonlinear wavetrain beyond x_{cs}; comparison of its slope with $-k_i^+(\omega_0^{ca}, x = 82) = -0.51$ and $-k_i^-(\omega_0^{ca}, x = 82) = 3$. (*c*) The instability balloon is presented (grey region) together with the linear spatial branches k_r^{l+} (solid curve) and k_r^{l-} (dashed curve) computed with $\omega_0 = \omega_0^{ca}$. Pinching occurs for the absolute wavenumber k_0^{ca} at $x = x_{ca}$ and $x = x_{ac}$. The dots in (*c*) represent local wavenumbers computed numerically.

(ii) that upstream of x_{ca}, the front displays the same slope as a k^- wave and that downstream of x_{cs} the nonlinear global mode decays as a k^+ wave; (iii) that the real wavenumber in the central region of the nonlinear global mode is connected downstream of x_{cs} to the real wavenumber of a k^+ wave.

Concerning the frequency selection process, figure 1(*a*) shows that for $Ra = 60$ and $Pe = 6$, the numerically computed global frequency is $\omega_g = 20.52$ to be compared with the theoretical value $\omega_0^{ca} = 20.355$. Moreover, numerical results displayed in figures 1(*c*) and 1(*e*) confirm that the global frequency criterion is still valid for varying Ra and Pe numbers. Next, we will examine the complete spatial structure of the nonlinear global mode. Specifically, we focus on the correlation of spatial branches determined by local stability analysis with both the observed sharp upstream front located in the vicinity of x_{ca} and the decaying nonlinear wavetrain beyond the spatial position x_{cs} (figure 2*a*). The spatial structure of the upstream front is illustrated in the semi-algorithmic diagram of figure 2(*b*). The linear spatial growth

https://doi.org/10.1017/S0022112007009159 Published online by Cambridge University Press

rates $-k_i^-(\omega_0^{ca})$ and $-k_i^+(\omega_0^{ca})$ evaluated at $x=-55$, a spatial position corresponding to a local convective instability in the upstream tail, are also shown in figure 2(*b*). We would like to point out that in the convectively unstable parameters, the complex spatial branches k^+ and k^- are associated with instability waves propagating in the downstream and upstream direction, respectively. Figure 2(*b*) clearly demonstrates that the slope of the global mode envelope is ruled by $-k_i^-(\omega_0^{ca})$ in the upstream convectively unstable region. Moreover, in the semi-logarithmic diagram of figure 2(*d*), the decaying nonlinear wavetrain beyond x_{cs} is seen to be ruled by the k^+ spatial growth rate. Therefore, we conclude that the spatial position x_{ca} plays a key role in generating global self-sustained oscillations independently of the presence of any persistent forcing of an initial perturbation. We now examine the connection between the numerically computed real wavenumbers and linear theory. Let us first recall that a region of instability is characterized by perturbations which amplify in time, starting from an initial spatially periodic perturbation, i.e. we assume that the perturbation wavenumber k is real while its frequency ω is complex. A positive temporal growth rate allows us to define an instability balloon in the (x, k)-plane (grey domain of figure 2(*c*) bounded by a contour where $\omega_i=0$. In our numerical simulations, we found a unique wavelength selection in the central region of the instability balloon. It depends only on the final $Pe-Ra$ combination. For $Ra=60$ and $Pe=6$, the dots in figure 2(*c*) indicate local wavenumbers obtained numerically by considering an average of local distances between eight adjacent rolls of the global mode (figure 2*a*). We also display in this figure the linear spatial branches k_r^{l+} (solid curve) and k_r^{l-} (dashed curve) computed with $\omega_0=\omega_0^{ca}$ in the complex k-plane. We observe from the (x, k)-plane of figure 2(*c*) that the nonlinear travelling waves exhibit a spatially uniform wavelength downstream of x_{ca} until the boundary x_{cs} of the instability balloon. At the neutrally stable location x_{cs}, the linear spatial branch k_r^{l+} takes over in the downstream linear region $x>x_{cs}$.

3.2. *Results in the case of an absolute instability region attached to the inlet*

This section aims at characterizing the properties of nonlinear global modes of mixed convection flows displaying a sufficiently extended region of absolute instability near the inlet of the porous cavity. For a set of parameters fixed in the fully nonlinear regime, direct numerical simulations demonstrate that, after transients, the solution is composed with a front connecting the conductive state at the inlet to synchronized oscillatory patterns downstream. In order to exemplify some properties of the observed nonlinear global mode, we present results of numerical resolutions corresponding to $Ra=52$ and $Pe=5$. Figure 3(*a*) illustrates the spatial structure of the nonlinear global mode which extends downstream beyond the neutrally stable station x_{cs}. This figure also shows that the maximum of the amplitude is located in the absolutely unstable region at a distance x_s from the inlet. In this regard, it is useful to recall the theoretical results obtained by Couairon & Chomaz (1999) within the Landau–Ginzburg model. These authors concentrate on scaling properties and frequency selection criterion relevant to unstable spatially developing flows in a semi-infinite domain. In particular, their model predicts that (i) the global mode frequency corresponds to the absolute frequency at the inlet in the limit of marginal global instability; (ii) the scaling law which links the characteristic length x_s to the departure from the threshold Ra^A of absolute instability is $x_s \approx (Ra-Ra^A)^{-1/2}$; (iii) the maximum A_s of the global mode amplitude follows the law $A_s \approx (Ra(x_s)-Ra_c)^{+1/2}$, where $Ra(x_s)$ and Ra_c are, respectively, the local Rayleigh number evaluated at $x=x_s$ and its value at the onset of convective instability. These theoretical predictions based on model equations are

https://doi.org/10.1017/S0022112007009159 Published online by Cambridge University Press

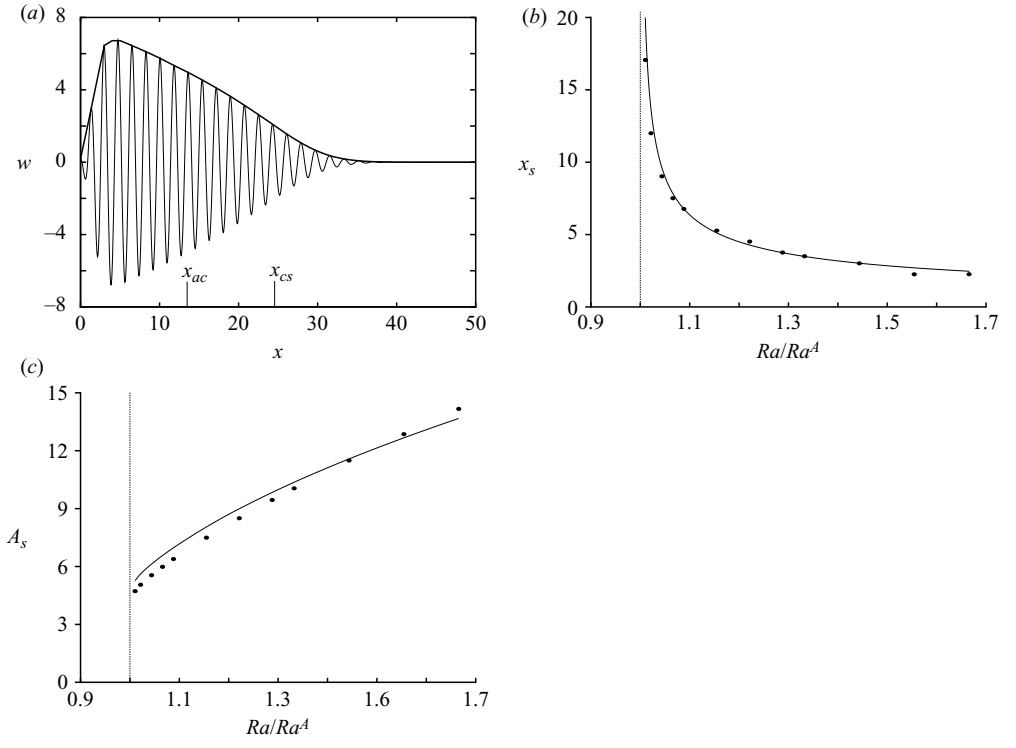

FIGURE 3. (*a*) Nonlinear global mode shape; the perturbation of the vertical velocity component in the middle of the semi-infinite porous medium is presented as a function of the downstream distance for $Pe = 5$ and $Ra = 52$. (*b*) Distance x_s from the inlet to the spatial position where the maximum of the nonlinear global mode occurs obtained by direct numerical simulations (dotted) for $Pe = 5$; this distance is fitted well by the expression $x_s = 3.9\pi(Ra - Ra^A)^{-1/2}$ (solid). (*c*) The maximum A_s of the global mode amplitude obtained numerically (dotted) which is fitted well by $A_s = 2.3(Ra(x_s) - Ra_c)^{+1/2}$ (solid).

compared to the results stemming from direct numerical simulations of the current problem. The frequency selection process is illustrated in figure 1(*b*) for $Ra = 52$ and $Pe = 5$. This figure shows that ω_g is nearly equal to $\omega_{0,r}$ ($x = 0$). In addition, numerical results displayed in figure 1(*d*) for varying Ra and $Pe = 5$ and in figure 1(*f*) for varying Pe and $Ra = 52$ confirm that this frequency selection criterion is still robust far from the threshold of marginal global instability. This result is not consistent with the theory of nonlinear global modes which allows for a linear departure between the global frequency and the absolute frequency at the inlet after the absolute instability threshold which, as for a wake (Chomaz 2003), is absent (figure 1*d*).

Finally, numerical runs show that the global mode steepens at the inlet as Ra increases beyond Ra^A. For $Pe = 5$, we find that the position x_s and the maximum A_s of the global mode amplitude are fitted well by the expressions $x_s = 3.9\pi(Ra - Ra^A)^{-1/2}$ (figure 3*b*) and $A_s = 2.3(Ra(x_s) - Ra_c)^{+1/2}$ (figure 3*c*), respectively, in agreement with the scaling laws derived in Couairon & Chomaz (1999).

4. Conclusions

A study combining linear spatio-temporal analysis and direct numerical simulations has been carried out here to explore the fully nonlinear solutions of mixed convection

https://doi.org/10.1017/S0022112007009159 Published online by Cambridge University Press

flows in porous media non-uniformly heated from below and subjected to a horizontal pressure gradient. The shape of the prescribed temperature at the bottom boundary is assumed to vary slowly in the through-flow direction. The result is the establishment of a weakly inhomogeneous basic state, the stability of which is carried out using the WKBJ approximation. Regions of local absolute instability are identified and the frequency of oscillating solutions is determined as a function of downstream position for two generic cases: the base flow displays a pocket of absolute instability bordered by two convective instability regions or the base flow promotes a finite region of absolute instability near the inlet of the medium. For both configurations, direct numerical simulations of the two-dimensional problem indicate that the presence of a region of absolute instability gives rise to nonlinear global modes in the form of self-sustained oscillations with well-defined frequency. It is found that the numerically computed frequency corresponds to the marginal absolute frequency in the case of a pocket of absolute instability and to the absolute frequency at the inlet if the base flow is absolutely unstable at the inlet. A close inspection of the spatial structure underlying these nonlinear global modes shows the following.

(i) In the case of a pocket of absolute instability, a nonlinear global mode is composed both by a sharp front located at the upstream boundary of absolute instability which decays upstream as a k^- wave and by a nonlinear wavetrain beyond the downstream convective/stable transition station which decays as a k^+ wave. This spatial structure corresponds to the steep global mode scenario described by Pier *et al.* (2001) and ascertains that the upstream station of marginal absolute instability acts as a generator of self-sustained oscillations.

(ii) In the case of an absolutely unstable region attached to the inlet, the scaling laws for the maximum of the global modes amplitude and for its spatial location agree perfectly with the predictions from model analyses in semi-infinite media (Couairon & Chomaz 1999).

We argue that mixed convection in porous media is a good candidate to describe global instabilities in open-flow systems. Therefore, we hope that the present theoretical contribution will stimulate much needed and desirable laboratory experiments with non-invasive techniques similar to those used by Shattuck *et al.* (1997) and Howle *et al.* (1997) in their work dealing with natural convection in porous media.

REFERENCES

Carrière, Ph. & Monkewitz, P. A. 1999 Convective versus absolute instability in mixed Rayleigh–Bénard–Poiseuille convection. *J. Fluid Mech.* **384**, 243–262.

Chomaz, J. M. 2003 Fully nonlinear dynamics of parallel wakes. *J. Fluid Mech.* **495**, 57–75.

Chomaz, J. M. 2005 Global instabilities in spatially developing flows: non-normality and nonlinearity. *Annu. Rev. Fluid Mech.* **37**, 357–392.

Combarnous, M. & Bories, S. A. 1975 Hydrothermal convection in saturated porous media. *Adv. Hydrosci.* **10**, 231–307.

Couairon, A. & Chomaz, J. M. 1999 Fully nonlinear global modes in slowly varying flows. *Phys. Fluids* **11**, 3688–3703.

Delache, A. Ouarzazi, M. N. & Combarnous M. 2007 Spatio-temporal stability analysis of mixed convection flows in porous media heated from below: comparison with experiments. *Intl J. Heat Mass Transfer* **50**, 1485–1499.

Dufour, F. & Néel, M. C. 1998 Numerical study of instability in a horizontal porous channel with bottom heating and forced horizontal flow. *Phys. Fluids* **10** (9), 2198–2207.

Goujon-Durand, S., Jenffer, P. & Wesfreid, J. E. 1994 Downstream evolution of the Bénard–von Kármán instability. *Phys. Rev.* E **50**, 308–313.

https://doi.org/10.1017/S0022112007009159 Published online by Cambridge University Press

Howle, L. E., Behringer, R. P. & Georgiadis, J. G. 1997 Convection and flow in porous media. Part 2. Visualization by shadowgraph. *J. Fluid Mech.* **332**, 247–262.

Huerre, P. A. & Monkewitz, P. A. 1990 Local and global instabilities in spatially developing flows. *Annu. Rev. Fluid Mech.* **22**, 473–537.

Leriche, E. & Labrosse, G. 2000 High-order direct Stokes solvers with or without temporal splitting: numerical investigations of their comparative properties. *SIAM J. Sci. Comput.* **22** 1386–1410.

Leriche, E. & Labrosse, G. 2007 Vector potential–vorticity relationship for the Stokes flows. Application to the Stokes eigenmodes in 2D/3D closed domain. *Theor. Comput. Fluid Dyn.* **21**, 1–13.

Lesshafft, L., Herre, P., Sagaut, P. & Terracol, M. 2006 Nonlinear global modes in hot jets. *J. Fluid Mech.* **554**, 393–409.

Marquillie, M. & Ehrenstein, U. 2003 On the onset of nonlinear oscillations in a separating boundary-layer flow. *J. Fluid Mech.* **490**, 169–188.

Monkewitz, P. A., Huerre, P. & Chomaz, J. M. 1993 Global linear stability analysis of weakly non-parallel shear flows. *J. Fluid Mech.* **251**, 1–20.

Ouarzazi, M. N., Bois, P. A. & Taki, M. 1996 Global stability analysis of transverse modes in laser systems under inhomogeous pumping. *Phys. Rev.* A **53**, 4408–4419.

Pier, B., Huerre, P. & Chomaz, J. M. 2001 Bifurcation to fully nonlinear synchronized structures in slowly varying medi. *Physica* D **148**, 49–96.

Pier, B. & Huerre, P. 2001 Nonlinear self-sustained structures and fronts in spatially developing wake flows. *J. Fluid Mech.* **435**, 145–174.

Shattuck, M. D., Behringer, R. P., Johnson, G. A. & Georgiadis, J. G. 1997 Convection and flow in porous media. Part 1. Visualization by magnetic resonance imaging. *J. Fluid Mech.* **332**, 215–245.

Zielinska, B. J. A. & Wesfreid, J. E. 1995 On the spatial structure of global modes in wake flow. *Phys. Fluids* **7**, 1418–1424.

https://doi.org/10.1017/S0022112007009159 Published online by Cambridge University Press